JOURNAL OF CATALYSIS 139, 602–610 (1993)

Vanadium Oxide Deposited on an Rh Foil: CO and CO_2 Hydrogenation Reactivity

A. B. BOFFA,* A. T. BELL,† AND G. A. SOMORJAI*

*Materials Sciences Division, Center for Advanced Materials, Lawrence Berkeley Laboratory, and Departments of *Chemistry and †Chemical Engineering, University of California, Berkeley, California 94720*

Received May 26, 1992; revised August 24, 1992

The effects of submonolayer deposits of vanadia on the rates of CO and CO_2 hydrogenation of an Rh foil have been examined. Auger electron spectroscopy (AES), ion scattering spectroscopy (ISS), and temperature-programmed desorption (TPD) have been used to determine the oxide coverage, and X-ray photoelectron spectroscopy (XPS) has been used to determine the oxidation state for VO_x deposits on a rhodium foil. After oxidation (3×10^{-6} O_2 at 350°C), the vanadium valence state is 3+, which corresponds to an oxide stoichiometry of V_2O_3. CO chemisorption reduces 34% of the V^{3+} to V^{2+} at low oxide coverages. The absolute amount of V^{2+} in the oxide overlayer after CO titration is found to maximize at a coverage of 0.5 ML. The rates of CO and CO_2 hydrogenation increase upon addition of VO_x to an Rh foil. For CO hydrogenation, the rate maximizes at two times that of the rate on the clean surface at an oxide coverage of 0.4 ML. For CO_2 hydrogenation, the rate maximizes at six times that of the clean surface rate at an oxide coverage of 0.6 ML. The oxide promoter also alters the activation energies, partial pressure dependences, and selectivities for the hydrogenation reactions. A comparison of the kinetic and spectroscopic data reveals a strong correlation between the degree of reducibility of the oxide overlayer and the amount of rate enhancement for CO and CO_2 hydrogenation.

INTRODUCTION

Numerous investigations have shown that interactions between small particles of Group VIII metal and metal oxide supports can result in a decoration of the metal particles by metal oxide moieties derived from the support (*1*, *2*). Originally, referred to as strong-metal–support-interactions (SMSI) when first reported by Tauster (*3*), this phenomenon has been the object of intense research. There are two principal reasons for interest in metal–metal oxide interactions. The first is that such interactions can result in a decrease in chemisorption capacity due to blockage of metal sites. The second reason is that metal–metal oxide interactions can give rise to very significant increases in catalyst activity, particularly for reactions such as CO and CO_2 hydrogenation and NO reduction (*1–5*).

The study of effects of metal–metal oxide interactions on the catalytic activity of supported metal catalysts is encumbered by difficulties in defining and controlling the extent of metal particle decoration by moieties derived from the support. Not only the method of catalyst preparation, but also the method of pretreatment (e.g., calcination and reduction condition) can affect the extent of decoration. To obtain greater experimental control, it is possible to produce a planar model catalyst in which a single crystal or foil is partially covered by vapor deposition of an oxide. Such samples can readily be characterized by a number of surface analytical techniques, and possess sufficient activity to enable studies of reaction kinetics. Experiments conducted with Rh, Pt, Ni, and Pd, decorated by several different oxides, have shown that planar model catalysts exhibit activities and selectivities very similar, and often identical, to those observed for metal oxide-supported metals

0021-9517/93 $5.00

(*6–10*). In one such study, the coverage dependence of the reactivity of a Rh foil promoted with deposits of TiO_x for CO and CO_2 hydrogenation were investigated (*11, 12*). It was found that addition of 0.5 ML of TiO_x to the Rh foil caused a rate enhancement of three times for CO hydrogenation and 15 times for CO_2 hydrogenation. The aim of the present investigation is to establish the effects of vanadia addition on the activity of Rh for CO and CO_2 hydrogenation. The observed changes in activity are correlated with measurements of oxide coverage and composition obtained by AES, ISS, TPD, and XPS.

EXPERIMENTAL

Experiments were performed in a Varian UHV chamber equipped with a cylindrical mirror analyzer for Auger electron spectroscopy, an EAI quadropole mass spectrometer, and an atmospheric-pressure isolation cell. Additional characterization of the catalyst samples were carried out in a PHI 5300 ESCA system equipped with X-ray photoelectron spectroscopy and ion scattering spectroscopy.

The Varian UHV chamber has been described in detail in Ref. (*13*). It is evacuated by an oil diffusion pump and titanium sublimation pump to achieve a base pressure of 1×10^{-9} Torr. The sample, 1-cm^2 Rh polycrystalline foil 0.002-in thick, is attached to a manipulator through spot welds to 0.020-in gold support wires. An S-type thermocouple is spot welded to the foil for temperature measurement. Prior to initiating a reaction, the foil is cleaned by high temperature annealing and sputtering to remove B, S contamination.

Vanadium was deposited on the Rh surface using an evaporator. The evaporator consists of a 0.030-in W wire around which is wound 0.005-in V wire. A current of 38 A was necessary to give a deposition rate of approximately 1.0 ML/min. A back pressure of 4×10^{-7} Torr of oxygen was present during evaporation in order to reduce carbon contamination. After V deposition, the surface was oxidized at 3×10^{-6} Torr of O_2 at 623 K for 5 min. To remove oxygen adsorbed on the exposed Rh surface, 2×10^{-7} Torr of CO was admitted into the chamber for 20 s, and the sample was then flashed to 673 K. After preparation, an Auger spectrum was taken to determine the oxide coverage and to confirm the sample cleanliness. The bare Rh surface was given the same gas exposures before reaction to eliminate the possibility of ascribing rate enhancements to pretreatment effects. When necessary, the deposited oxide was removed by sputtering and annealing.

To perform a reaction, the sample was enclosed in a high-pressure cell, connected to a gas recirculation loop. The total volume of the reactor and recycle loop is 120 cm^3. H_2 and CO, or CO_2, purified through a trap maintained at 150 K, were introduced into the loop, and argon was added when necessary to give a total pressure of 760 Torr. A metal-bellows pump was used to recirculate the gases at a flow rate of approximately 100 cm^3/min. The accumulation of reaction products in the loop was monitored with an HP 5720A gas chromatograph equipped with an FID. A stainless steel 10 ft. × 1/8 in column packed with 80/120 Carbopak B coated with 3% SP1500 was used for product separation. All reactions were run at conversions of less than 5%. After reaction, approximately 10 min was required to return the UHV chamber to its base pressure.

The PHI ESCA 5300 was used for the XPS and ISS studies. It is equipped with an Mg and Al anode X-ray source, an He and Ar differentially pumped ion gun, a hemispherical analyzer, and a sample preparation cell. For XPS, the Mg anode (1253.6 eV) was used, and the hemispherical analyzer detector was operated at a 35.75-eV pass energy. For ISS, an incident beam of He ions at 500 eV was scattered at an angle of 123.0° and detected with the hemispherical analyzer operated at a 179-eV pass energy. Before analysis, catalyst samples were prepared in an adjacent preparation chamber which was maintained at a base pressure of

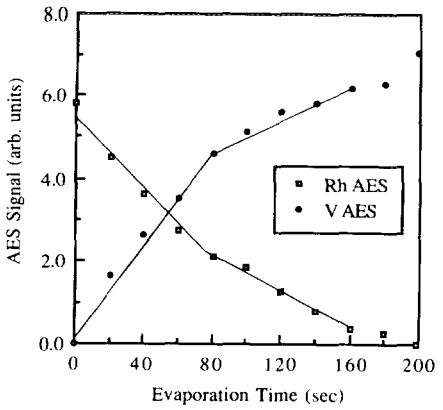

FIG. 1. Rh (302 eV) and V (435 eV) AES intensities as a function of vanadium evaporation time.

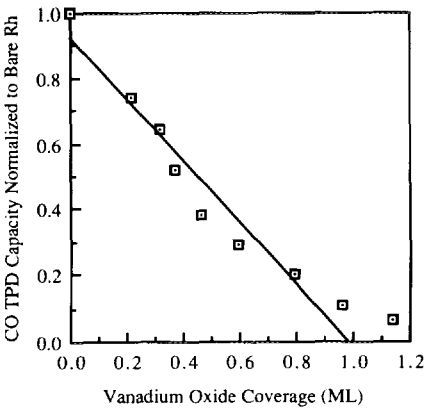

FIG. 2. CO TPD peak intensity as a function of vanadium oxide coverage.

2×10^{-8} Torr. A transfer rod was employed to move the sample between chambers *in vacuo*. An electron beam heater and a vanadium evaporation source were utilized to deposit vanadium oxide overlayers on an Rh foil surface in a similar manner as was described above for oxide preparation in the Varian UHV system.

RESULTS AND DISCUSSION

Sample Characterization

The coverage and growth mode for VO_x deposited on the Rh foil were determined by AES, ISS, and CO TPD, and the oxidation state of the vanadium was determined by XPS. Since all four techniques could not be carried out in one vacuum chamber, samples were produced in each of the two vacuum chambers, using identical procedures. The sample in the Varian UHV chamber was characterized by AES and CO TPD, whereas that in the PHI UHV chamber was characterized by ISS and XPS.

Figure 1 is a plot of the vanadium (435 eV) and rhodium (302 eV) AES peak intensities as a function of the vanadium evaporation time, in the Varian UHV chamber. Changes in the slopes of the plots of Rh and V peak intensity are observed after 80 s of V deposition.

Figure 2 shows a plot of CO TPD peak intensity as a function of VO_x coverage. The VO_x coverage has been determined using the coverage calibration derived from the AES uptake curve in Fig. 1. The addition of vanadium oxide to Rh causes a linear decline in CO TPD intensity with complete suppression at coverages of 1.0 ML or greater. Since CO does not adsorb appreciably on vanadia, the linear decline and complete suppression of the TPD peak intensity indicates that the AES coverage calibration correctly determines the amount of vanadium oxide on the surface.

Figure 3 shows a plot of Rh ISS intensity

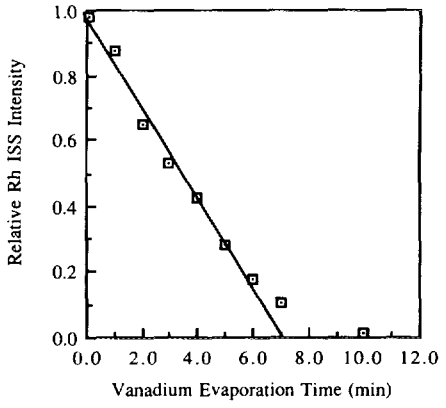

FIG. 3. Rh ISS intensity as a function of vanadium evaporation time.

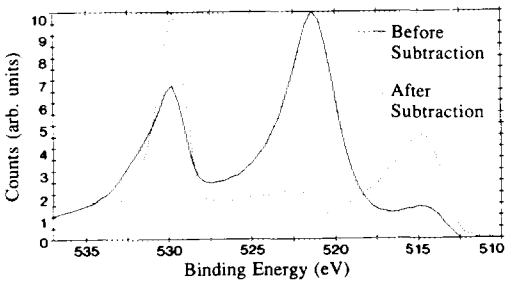

FIG. 4. XPS spectrum of 1.0 ML vanadium oxide deposit on Rh.

as a function of vanadium evaporation time in the PHI UHV chamber. The Rh ISS peak intensity decreases linearly with V evaporation time consistent with the growth of a two-dimensional film. A small degree of tailing occurs near 1.0 ML vanadium oxide coverage indicating that a second layer of vanadium oxide starts to form before completion of the first layer. After 7 min of vanadium evaporation, the relative Rh ISS intensity is less than 10% and the uptake curve begins to level off. Consequently, 7 min evaporation time is considered to be the point at which the Rh surface is covered by 1.0 ML. To determine the similarity of the VO_x overlayers produced in the PHI and Varian chambers, an AES measurement was made in the PHI chamber using the XPS spectrometer. For a V deposition time corresponding to 1.0 ML in both chambers, the Rh AES signal attenuation is 0.734 in the PHI chamber and 0.726 in the Varian chamber. The close agreement between these two values indicates that the two samples are similar.

An XPS spectrum of the 540 to 510 eV binding energy region for a 1.0-ML deposit of vanadium oxide on a Rh foil is shown in Fig. 4 (solid curve). The dominant features are the O(1s) peak at 529.8 eV and the Rh($3p1/2$) peak at 523.0 eV. The V($2p3/2$) at approximately 515 eV appears as a shoulder on the Rh($3p1/2$) peak. The dashed curve in Fig. 4 is a plot of the difference between the XPS spectra of an Rh surface covered by 1.0 ML of VO_x and a clean Rh surface.

XPS spectra were obtained at several different vanadium oxide coverages. At each coverage, the surface was oxidized with 3×10^{-6} Torr O_2 at 623 K for 5 min after which an XPS spectrum was recorded. The vanadium binding energy after the oxidation step remains the same, 515.6 eV, for all coverages. The measured V($2p3/2$) B.E. of 515.6 eV is identical to that measured for a sample of polycrystalline V_2O_3 pressed into a Ta mesh and is consistent with the B.E. reported in the literature for V_2O_3 (*14*, *15*), indicating that V in the fully oxidized overlayer is in the V^{3+} valence state.

After oxidation, the same sample was titrated with a saturation dose (10 liter) of CO, and a second XPS spectrum was taken. The vanadium B.E. after CO titration varies as a function of coverage. Figure 5 shows the percentage of the VO_x overlayer that is reduced from V^{3+} to V^{2+} after CO titration. The amount of V^{2+} was determined by subtracting the XPS spectrum of the fully oxidized V_2O_3 overlayer from that of overlayer reduced by CO titration. The resulting difference spectrum has a peak centered at 513.8 eV, which is taken to correspond to vanadium in the 2+ valence state (*15*). The percentage of V^{2+} in the overlayer decreases from 34% at 0.2 ML to less than 5% at coverages greater than 1.0 ML. This trend

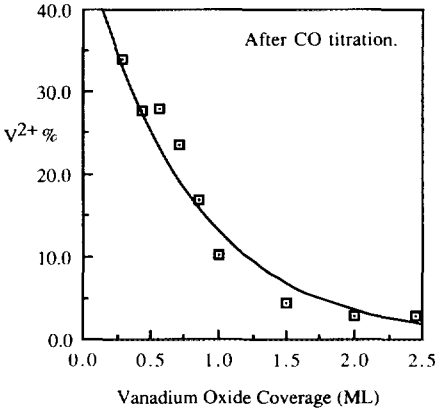

FIG. 5. V^{2+}% after CO titration as a function of vanadium oxide coverage.

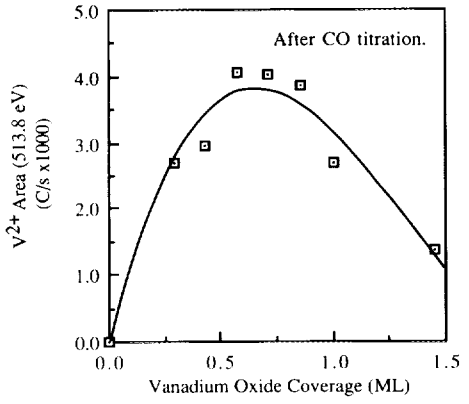

FIG. 6. Area of V^{2+} XPS (513.8 eV) peak as a function of vanadium oxide coverage.

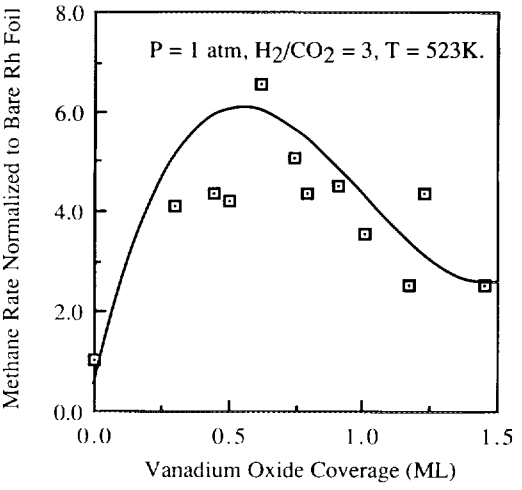

FIG. 7. Rate of methane formation of an Rh foil as a function of vanadium oxide coverage for CO hydrogenation.

is similar to that reported by Levin *et al.* (*16*) for TiO_x deposited on a Rh foil. These authors found that CO titration reduced 40% of the titanium from Ti^{4+} to Ti^{3+} at low coverages, whereas at higher coverages, CO titration had almost no effect. Figure 6 shows the absolute amount of V^{2+} in the overlayer after CO titration plotted as a function of coverage. The amount of V^{2+} is shown to maximize at coverages of VO_x of approximately 0.5 ML.

An explanation for the observation that the degree of reduction of the oxide overlayer decreases with increasing coverage becomes apparent when the CO uptake curve is considered. Figure 2 shows that CO does not adsorb appreciably on the vanadium oxide overlayer; therefore, at coverages greater than 1.0 ML, Rh adsorption sites are completely blocked, and the oxide overlayer is unaffected by CO titration. However, as the coverage decreases, more Rh adsorption sites are exposed, and the oxide is readily reduced. These results suggest that reduction of the vanadia overlayer occurs via diffusion of CO adsorbed on the exposed Rh sites to the perimeter of the vanadia islands comprising the overlayers.

Catalytic Activity

The rate of methane formation over the unpromoted Rh foil is 0.034 s^{-1} for CO hydrogenation at 553 K in the presence of 253 Torr CO and 506 Torr H_2, and 0.19 s^{-1} for CO_2 hydrogenation at 523 K in the presence of 190 Torr CO_2 and 570 Torr H_2. As shown in Figs. 7 and 8, promotion with VO_x has a significant effect on the rate of CH_4 formation from both CO and CO_2. For CO hydrogenation, the rate increases to a maximum of twice that for the clean surface, for a

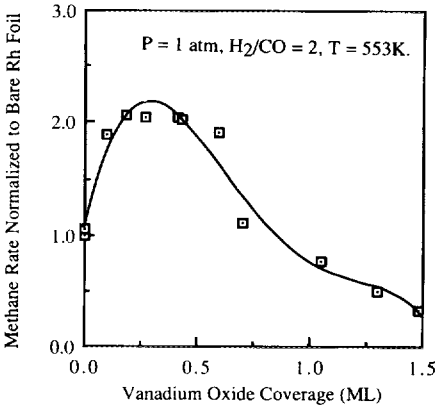

FIG. 8. Rate of methane formation of an Rh foil as a function of vanadium oxide coverage for CO_2 hydrogenation.

TABLE 1

Comparison between CO and CO_2 Hydrogenation Kinetics over Clean and VO_x-Covered Rh Foil

	CO + H_2		CO_2 + H_2	
	Clean Rh	0.5 ML VO_x	Clean Rh	0.5 ML VO_x
CH_4 act. energy, E_a (kcal/mol)	24	13	17	13
H_2 pressure exponent, a	1.0	2.1	0.5	0.3
CO/CO_2 pressure exponent, b	−1.0	−0.7	0.2	0.2
Selectivity to CH_4 (%)	90	65	99+	99+
Normalized rate	1.0	0.7	1.0	6.0

VO_x coverage of 0.4 ML, whereas for CO_2 hydrogenation, the rate increases six times that for the clean surface, for a VO_x coverage of 0.6 ML. The 0.2-ML difference in the VO_x coverages at the rate maxima for CO and CO_2 hydrogenation could be explained by postulating a change in oxide morphology resulting from the difference in vanadium valence states present during the two reactions (see Table 2). However, the lack of direct structural information makes any comment on the significance of this small difference in coverages speculative. AES and XPS characterization of the catalyst after CO or CO_2 hydrogenation indicate the presence of carbon on the surface, the amount being twofold greater for CO hydrogenation than for CO_2 hydrogenation. For both reactions, though, promotion of Rh with 0.5 ML VO_x increases the amount of carbon deposited.

The rate parameters for CH_4 formation from CO and CO_2 hydrogenation over clean and VO_x covered Rh are presented in Table 1. The rate of CH_4 formation is assumed to be given by a power-law expression of the form

$$r_{CH_4} = k_0 \exp(-E_a/RT) P_{H_2}^a P_{CO_x}^b),$$

where E_a, a, and b represent the activation energy, hydrogen partial pressure dependence, and CO or CO_2 partial pressure dependence, respectively. For the determination of E_a, four rate measurements were made over a range of temperatures from 250 to 400°C. For the determination of the parameter a, three measurements were made over a range of pressures from 169 to 590 Torr, and for the parameter b, three measurements were made over a range of pressures from 63 to 253 Torr. For CO hydrogenation, E_a = 24 kcal/mol over the clean Rh surface. Upon promotion with vanadium oxide, E_a decreases to 13 kcal/mol. The values of a and b for the clean surface are 1.0 and −1.0, respectively. Promotion with vanadium oxide increases a to 2.1 and b to −0.7. For CO_2 hydrogenation, addition of vanadium oxide decreases E_a from 17 to 13 kcal/mol. However, addition of vanadium oxide has no effect on a and b. Similar changes in rate parameters have been observed for TiO_x on an Rh foil (*11*, *12*) and for $Rh/V/SiO_2$ (*17*).

Selectivities of the clean and VO_x covered surface are also presented in Table 1. The selectivity toward methane formation from CO decreases from 90 to 67% upon promotion with 0.5 ML VO_x, and the selectivities for ethylene, ethane, and propylene increase from 3.7, 3.3, and 1.6%, respectively, to 17, 2.5, and 8.0%, respectively. In contrast to CO hydrogenation, VO_x promotion has no effect on the selectivity for CO_2 hydrogenation. With and without VO_x present the selectivity to CH_4 is 99+%.

The effects of VO_x promotion on the rate of CH_4 formation from CO and CO_2 over Rh presented here are similar to those reported earlier for TiO_x. Levin *et al.* (*11*) observed a threefold increase in the rate of CO hydrogenation, when an Rh foil was promoted with 0.5 ML of TiO_x, and Williams *et al.* (*12*) observed a 15-fold increase in the rate of CO_2 hydrogenation, also for a TiO_x coverage on Rh of 0.5 ML. Also relevant is the work of van Santen and co-workers (*17*), who found that promotion of a Rh/SiO_2 catalyst with an amount of VO_x sufficient to decrease the CO chemisorption capacity by 50% in-

creases the CO hydrogenation activity of the catalyst fourfold.

Previous studies have suggested that the mechanisms for CO and CO_2 hydrogenation are similar (*18*). In both instances the critical step is cleavage of the C–O bond in adsorbed CO or a CH_xO ($x \leq 3$) species, the origin of adsorbed CO in the case CO_2 hydrogenation being the dissociation of CO_2 (*19–23*). The C_s or $CH_{x,s}$ species released by C–O bond cleavage of CO or CH_xO readily undergo hydrogenation to form CH_4. In support of this picture, it has been observed that adsorbed CO does not dissociate appreciably on Rh(111) surfaces (*24*) and that during temperature-programmed reduction of adsorbed CO by H_2, CH_4 and H_2O appear concurrently (*17*). Studies with Rh/SiO_2 indicate, as well, that the rate constant for CO dissociation is considerably smaller than that for CH_x hydrogenation (*21*).

The increase in CO methanation activity when Rh is promoted with VO_x correlates very closely with the amount of deposited V present in the 2+ state, as can be seen by comparing Figs. 6 and 7. Since reduction of the deposited oxide proceeds inward from the metal–oxide adlineation (*25*), a significant fraction of the V^{2+} cations are expected to be present at the perimeter of the VO_x islands comprising the overlayer. CO molecules can adsorb at these boundaries in such a fashion that the C end of the molecule is bound to an exposed Rh atom, while the O end of the molecule is bound to a V^{2+} cation. Such bonding has been postulated earlier to facilitate cleavage of the C–O bond (*26–28*). Thus, it is hypothesized that the observed increase in the methanation rate is attributable to the increased rate of CO dissociation caused by the presence of V^{2+} cations. Consistent with this interpretation are the AES and XPS observations that VO_x promotion increases the concentration of surface carbon produced during CO hydrogenation.

The changes in the rate parameters for CO hydrogenation when Rh is promoted with VO_x (see Table 1) can also be explained in the light of the postulated model. Williams *et al.* (*29*) have shown that greatly increasing the rate of dissociation of adsorbed CO by addition of an oxide promoter ultimately results in a shift in the rate limiting step from CO dissociation to hydrogenation of CH_x species. Such a shift causes an increase in the apparent dependence of the methanation rate on the partial pressure of H_2, and a decrease in the apparent dependence on the CO partial pressure.

The increase in the rate of CO_2 hydrogenation also correlates with the amount of V^{2+} present on the Rh surface, in a manner similar to that observed for CO hydrogenation. However, in contrast to CO hydrogenation, the maximum rate enhancement is much greater. Inspection of Table 2 also shows that the percentage of V^{2+} in a 0.5-ML VO_x overlayer is greater following CO_2 than CO hydrogenation. The greater amount of V^{2+} in the former case can be attributed to a higher surface coverage by atomic H, a reducing agent that is more effective than CO in attacking VO_x, since CO_2 adsorbs much more weakly than CO, and, hence, will not inhibit the dissociative adsorption of H_2 on Rh. V^{2+} cations are expected to enhance both the rate of CO_2 dissociation to CO and the rate of CO dissociation to C and O. The absence of a change in the H_2 and CO_2 partial pressure dependences of the rate of CO_2 methanation upon VO_x promotion suggests that the rate-limiting step is unaffected by the presence of the promoter.

To further emphasize the correlation between rate enhancement and reducibility, the data contained in Figs. 6, 7, and 8 are replotted in Fig. 9 as methanation rate versus V^{2+} XPS peak area for various oxide coverages. For CO_2 hydrogenation, the data fit to a linear function, indicating that the degree of rate enhancement depends directly on the amount of reduced oxide. Although the CO hydrogenation data has more scatter, a qualitatively similar relationship exists between rate enhancement and oxide reducibility. The linear correlation of rate enhancement and oxide reducibility illustrated in Fig. 9 provides direct support for

TABLE 2

Percentage of V^{2+} in the VO_x Overlayer Following CO Titration, and CO and CO_2 Hydrogenation

Treatment	1×10^{-6} Torr O_2 at 623 K and 5×10^{-7} Torr CO at 523 K	200 Torr H_2 and 50 Torr CO at 523 K for 60 min	200 Torr H_2 and 50 Torr CO_2 at 523 K for 60 min
VO_x coverage (ML)	0.5	0.5	0.5
% V^{2+}	28	54	98

the often postulated mechanism (*11, 26–28*) involving active site formation at reduced oxide sites of the oxide/metal interface and suggests that a redox interaction between the metal ion valence states ($V^{2+} - V^{3+}$) of the oxide promoter and the CO(a) reaction intermediates facilitates CO bond cleavage and leads to an increase in methanation rate. Assuming such a scheme is valid, the promoter effectiveness of different oxides will depend not only on the number of reduced oxide sites, but also on the redox potential of the metal ion valence pair.

CONCLUSIONS

Vanadia deposited on an Rh foil forms a two-dimensional overlayer at coverages below 1 ML. In the fully oxidized state, vanadium in the overlayer is present as V^{3+}. Titration of the O atoms present on the Rh surface reduces the V^{3+} cations in the overlayer to V^{2+}, the amount of V^{2+} cations passing through a maximum at a VO_x coverage of 0.5 ML.

The deposits of vanadium oxide cause rate enhancements for CO and CO_2 hydrogenation. For CO hydrogenation, the rate maximizes at two times that of the clean surface rate at a coverage of 0.4 ML. For CO_2 hydrogenation, the rate maximizes at 6 times that of the clean surface rate at a coverage of 0.6 ML. For CO hydrogenation, the oxide promoter also causes a decrease in the activation energy, an increase in hydrogen partial pressure dependence, and an increase in selectivity to higher weight hydrocarbons. For CO_2 hydrogenation, the oxide has little effect on activation energy and partial pressure dependences. The strong correlation between the amount of V^{2+} cations present and the rates of CO and CO_2 hydrogenation as a function of coverage suggests that V^{2+} cations are responsible for increasing the rates of methane formation. It is proposed that V^{2+} cations promote the dissociation of CO_2 to CO_s and O_s, and of CO to C_s and O_s. The latter reaction, in particular, is hypothesized to be critical for the synthesis of methane from CO or CO_2.

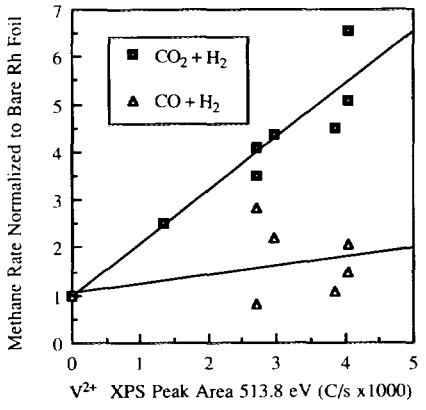

FIG. 9. Rate of methane formation for CO and CO_2 hydrogenation as a function of V^{2+} XPS (513.8 eV) peak area for various vanadium oxide coverages on an Rh foil.

ACKNOWLEDGMENTS

This work was supported by the Director, Office of Energy Research, Office of Basic Energy Sciences, Materials Sciences Division of the U.S. Department of Energy under Contract DE-AC03-76SF00098.

REFERENCES

1. Bell, A. T., *in* "Catalyst Design—Progress and Perspectives" (L. L. Hegedus, Ed.), Wiley, New York, 1987.
2. Haller, G. L., and Resasco, D. E., *Adv. Catal.* **36,** 173 (1989).
3. Tauster, S. J., *Acc. Chem. Res.* **20,** 389 (1987).
4. Iizuka, T., Tanaka, Y., and Tanabe, K., *J. Catal.* **76,** 1 (1982).
5. Pande, N. T., and Bell, A. T., *J. Catal.* **98,** 7 (1986).
6. Chung, Y.-W., Xiong, G., and Kao, C. C., *J. Catal.* **85,** 237 (1984).
7. Demmin, R. A., Ko, C. S., and Gorte, R. J., *J. Phys. Chem.* **89,** 1151 (1985).
8. Demmin, R. A., and Gorte, R. J., *J. Catal.* **98,** 577 (1986).
9. Levin, M. E., Salmeron, M., Bell, A. T., and Somorjai, G. A., *J. Chem. Soc. Faraday Trans. 1* **83,** 2061 (1987).
10. Demmin, R. A., and Gorte, R. J., *J. Catal.* **105,** 373 (1987).
11. Levin, M. E., Salmeron, M., Bell, A. T., and Somorjai, G. A., *J. Catal.* **106,** 401 (1987).
12. Williams, K. J., Boffa, A. B., Lahtinen, J., Salmeron, M., Bell, A. T., and Somorjai, G. A., *Catal. Lett.* **5,** 385 (1990).
13. Levin, M. E., Salmeron, M., Bell, A. T., and Somorjai, G. A., *Surf. Sci.* **169,** 123 (1986).
14. Lars, S., and Anderson, T., *J. Chem. Soc. Faraday Trans. 1* **75,** 1356 (1979).
15. Sexton, B. A., Hughes, A. E., and Foger, K., *J. Catal.* **77,** 85 (1982).
16. Levin, M. E., Salmeron, M., Bell, A. T., and Somorjai, G. A., *Surf. Sci.* **195,** 429 (1988).
17. Koerts, T., Welters, W. J. J., and van Santen, R. A., *J. Catal.* **134,** 1 (1992).
18. Henderson, M. A., and Worley, S. D., *J. Phys. Chem.* **89,** 1417 (1985).
19. Rieck, J. S., and Bell, A. T., *J. Catal.* **96,** 88 (1985).
20. Shustorovich, E., and Bell, A. T., *J. Catal.* **113,** 341 (1988).
21. Mori, T., Masuda, H., Imai, H., Miyamoto, A., Hasebec, R., and Murakami, Y., *J. Phys. Chem.* **87,** 3648 (1983).
22. Mori, T., Miyamoto, A., Niizuma, H., Takahashi, N., Hattori, T., and Murakami, Y., *J. Phys. Chem.* **90,** 109 (1986).
23. Mori, T., Miyamoto, A., Niizuma, H., Takahashi, N., Hattori, T., and Murakami, Y., *J. Phys. Chem.* **93,** 2039 (1989).
24. Castner, D. G., Sexton, B. A., and Somorjai, G. A., *Surf. Sci.* **71,** 519 (1978).
25. Wang, H. C., Ogletree, D. F., and Salmeron, M. B., *J. Vac. Sci. Technol. B* **9**(2), 853 (1991).
26. Sachtler, W. M. H., Shriver, D. F., Hollenberg, W. B., and Lang, A. F., *J. Catal.* **92,** 429 (1985).
27. Fukuoka, A., Kimura, T., Rao, L-F., and Ichikawa, M., *Catal. Today* **6,** 55 (1989).
28. Ichikawa, M., and Fukushima, T., *J. Phys. Chem.* **89,** 1564 (1985).
29. Williams, K. J., Boffa, A. B., Salmeron, M., Bell, A. T., and Somorjai, G. A., *Catal. Lett.* **9,** 41 (1991).